European Congress on Computational Methods in Applied Sciences and Engineering
ECCOMAS 2000
Barcelona, 11-14 September 2000

CONDITIONS OF UNIQUENESS FOR FINITE ELEMENTS WITH EMBEDDED CRACKS

Milan Jirásek

Laboratory of Structural and Continuum Mechanics (LSC)
Department of Civil Engineering (DGC)
Swiss Federal Institute of Technology (EPFL)
CH-1015 Lausanne, Switzerland
E-mail: Milan.Jirasek@epfl.ch
Web page: http://dgcwww.epfl.ch/WWWLSC/jirasek.page

Key words: Enriched Finite Elements, Displacement Discontinuities, Uniqueness, Localization, Cracking, Fracture.

Abstract. *The recently emerged idea of incorporating strain or displacement discontinuities into standard finite element interpolations has triggered the development of powerful techniques that allow efficient modeling of regions with highly localized strains, e.g. of fracture process zones in concrete or shear bands in metals or soils. The present paper addresses the fundamental issue of uniqueness of such enriched formulations, which has important implications for the robustness of the corresponding numerical algorithms. For a linear triangular element with an embedded strong discontinuity described by traction-separation law formulated within the framework of damage or plasticity, explicit conditions that guarantee uniqueness on the element level are derived, and the resulting restrictions limiting the size of the element are discussed.*

1 INTRODUCTION

Standard finite element approximations cannot properly capture the discontinuous character of the displacement field corresponding to localized fracture. In the context of smeared-crack models, this deficiency can lead to a spurious stress transfer across a widely open crack [1]. Discrete-crack models with special interfaces between conventional elements [2, 3, 4] do not suffer by this pathology, but they require frequent remeshing in order to allow for crack propagation in the correct direction. An elegant technique that combines the advantages of both approaches inserts a discontinuity into the interior of a finite element. The discontinuity can have an arbitrary orientation, which makes it much easier to capture a propagating crack or softening band without remeshing. This class of methods, collectively called *elements with embedded discontinuities*, has been inspired by the pioneering work of Ortiz et al. [5] and Belytschko et al. [6]. The early works dealt with weak (strain) discontinuities, but later the idea was extended to strong (displacement) discontinuities [7, 8, 9, 10].

A systematic classification and critical evaluation of such models within a unified framework has been presented in [11, 12, 13], with the conclusion that there exist three main groups of approaches, called statically optimal symmetric (SOS), kinematically optimal symmetric (KOS), and statically and kinematically optimal nonsymmetric (SKON). The SOS formulation works with a natural stress continuity condition, but it does not properly reflect the kinematics of a completely open crack. On the other hand, the KOS formulation describes the kinematic aspects satisfactorily, but it leads to an awkward relationship between the stress in the bulk of the element and the tractions across the discontinuity line.

The present study focuses on the nonsymmetric SKON formulation, which uses a very natural stress continuity condition and is capable of properly representing complete separation at late stages of the fracturing process. The aim is to derive criteria that guarantee uniqueness of the response on the element level, which is a necessary condition for robustness of the numerical algorithm. Section 2 gives a brief review of the basic kinematic and static equations for a constant-strain triangle with an embedded strong discontinuity. Section 3 presents a traction-separation law for the discontinuity (fictitious crack), postulated in the damage format. Uniqueness of the solution is analyzed in Section 3.2, and the resulting restrictions on the element size are derived in Section 3.3. The analysis is repeated in Section 4 for a traction-separation law in the format of plasticity.

2 ELEMENT WITH EMBEDDED DISPLACEMENT DISCONTINUITY

The first publication on elements with embedded discontinuities that combined the optimal static and kinematic equations is due to Dvorkin et al. [7], even though this aspect was not particularly emphasized in that paper. A very similar quadrilateral element was constructed by Klisinski et al. [8], based on simple and instructive physical considerations. In a later paper [9], the same technique was applied to a constant-strain triangle. A general

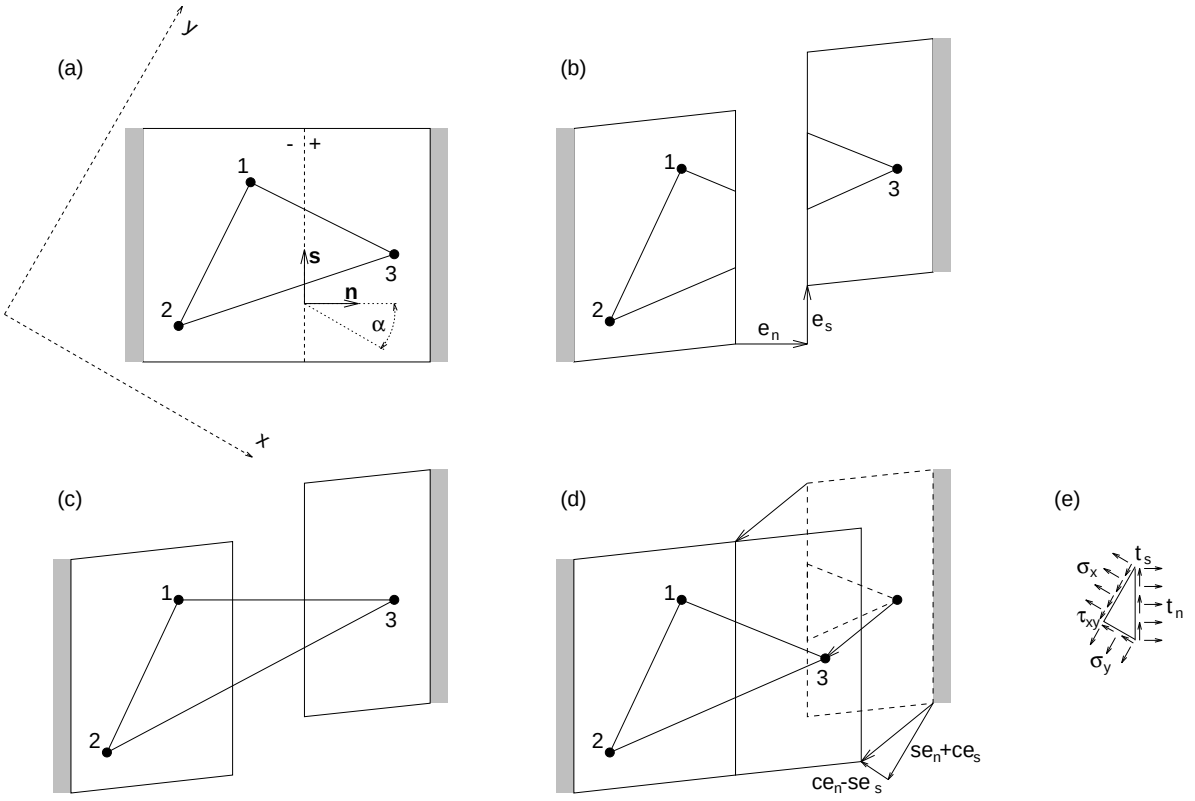

Figure 1: CST element with an embedded displacement discontinuity

version of the SKON formulation for an arbitrary type of parent element was outlined in a short paper by Simo and Oliver [10] and fully described by Oliver [14].

In the present study, we look at the triangular element first proposed by Olofsson et al. [9]; see Fig. 1a. The basic idea is that the displacement field is decomposed into a continuous part and a discontinuous part due to the opening and sliding of a crack (Fig. 1b). The same decomposition applies to the nodal displacements of a finite element. Instead of smearing the displacement jump over the area of the element and replacing it by an equivalent inelastic strain, as is done by standard smeared crack models (Fig. 1c), we represent the discontinuity by additional degrees of freedom, collected in a column matrix $\boldsymbol{e}$. The contribution of crack opening and sliding is then subtracted from the nodal displacement vector, $\boldsymbol{d}$, and only the part of the nodal displacements produced by the continuous deformation serves as input for the evaluation of strains in the bulk material, $\boldsymbol{\varepsilon}$; see Fig. 1d. This leads to kinematic equations in the form

$$\boldsymbol{\varepsilon} = \boldsymbol{B}(\boldsymbol{d} - \boldsymbol{H}\boldsymbol{e}) \tag{1}$$

where $\boldsymbol{\varepsilon} = \{\varepsilon_x, \varepsilon_y, \gamma_{xy}\}^T$ is the column matrix of engineering strain components, $\boldsymbol{B}$ is the standard strain-displacement matrix, and $\boldsymbol{H}$ is a matrix reflecting the effect of the displacement jump $\boldsymbol{e}$ (crack opening and sliding) on the nodal displacements.

In general, the displacement jump is approximated by a suitable function, for example a polynomial one. It is easy to show that the approximation need not be continuous on inter-element boundaries. For triangular elements with a linear displacement interpolation, the strains and stresses in the bulk are constant in each element, and so it is natural to approximate the displacement jump also by a piecewise constant function. In each element, the jump is described by its normal (opening) component, e_n, and tangential (sliding) component, e_s. These additional degrees of freedom have an internal character and can be eliminated on the element level, which means that the global equilibrium equations are written exclusively in terms of the standard unknowns—nodal displacements. From Fig. 1d it is clear that the crack-effect matrix is given by

$$\boldsymbol{H} = \begin{bmatrix} 0 & 0 \\ 0 & 0 \\ 0 & 0 \\ 0 & 0 \\ c & -s \\ s & c \end{bmatrix} \tag{2}$$

provided that the discontinuity line separates node 3 from nodes 1 and 2 (in local numbering). In (2), $c = \cos\alpha$ and $s = \sin\alpha$, where α is the angle between the normal to the crack (discontinuity line) and the global x-axis; see Fig. 1a.

Strains in the bulk material generate certain stresses, $\boldsymbol{\sigma} = \{\sigma_x, \sigma_y, \tau_{xy}\}^T$, which are here computed from the equations of linear elasticity,

$$\boldsymbol{\sigma} = \boldsymbol{D}_e \boldsymbol{\varepsilon} \tag{3}$$

where $\boldsymbol{D}_e$ is the elastic stiffness matrix (for plane stress or plane strain). Note that, in general, the constitutive law for the bulk material could be nonlinear. The tractions transmitted by the crack, $\boldsymbol{t}$, are linked to the separation vector (displacement jump) by another constitutive law that describes the gradual development of a stress-free crack. Specific forms of this law will be given in Sections 3 and 4.

The stresses in the bulk and the tractions across the crack must satisfy certain conditions that express internal equilibrium and serve as static equations corresponding to the internal degrees of freedom, $\boldsymbol{e}$. The most natural requirement is that the traction vector be equal to the stress tensor contracted with the crack normal, similar to static boundary conditions. This internal equilibrium (traction continuity) condition can be derived from equilibrium of an elementary triangle with one side on the discontinuity line; see Fig. 1e. In the engineering notation it reads

$$\boldsymbol{P}^T \boldsymbol{\sigma} = \boldsymbol{t} \tag{4}$$

where

$$\boldsymbol{P} = \begin{bmatrix} c^2 & -cs \\ s^2 & cs \\ 2cs & c^2 - s^2 \end{bmatrix} \tag{5}$$

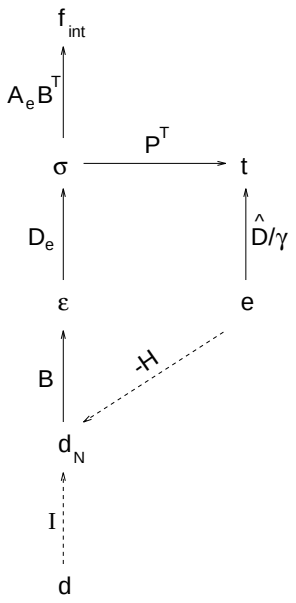

Figure 2: Structure of the equations describing the CST element with an embedded displacement discontinuity (SKON formulation)

is a stress rotation matrix. For linear triangles with a constant displacement jump, both $\boldsymbol{t}$ and $\boldsymbol{\sigma}$ are constant in each element, and so condition (4) can be satisfied exactly. In general it would have to be enforced in a weak sense. Finally, the nodal forces are evaluated from the standard relation

$$\boldsymbol{f}_{int} = A_e \boldsymbol{B}^T \boldsymbol{\sigma} \tag{6}$$

where A_e is the area of the element.

The structure of the basic equations describing a CST element with an embedded displacement discontinuity is schematically depicted in Fig. 2. Dashed arrows indicate that the source is added to the target, while solid arrows mean that the source must be equal to the target.

Substituting into the traction continuity condition (4) from (3) and (1), we obtain a useful expression for the traction vector in terms of the kinematic variables,

$$\boldsymbol{t} = \boldsymbol{P}^T \boldsymbol{D}_e \boldsymbol{B}(\boldsymbol{d} - \boldsymbol{H}\boldsymbol{e}) = \boldsymbol{A}(\boldsymbol{d} - \boldsymbol{H}\boldsymbol{e}) \tag{7}$$

where we have denoted

$$\boldsymbol{A} = \boldsymbol{P}^T \boldsymbol{D}_e \boldsymbol{B} \tag{8}$$

3 DAMAGE-TYPE TRACTION-SEPARATION LAW

3.1 Model Formulation

The basic equations presented in the preceding section must be completed by a law that links the traction transmitted by the discontinuity to the displacement jump. One possible type of such a law has been proposed in [15] in the form

$$\gamma \boldsymbol{t} = \hat{\boldsymbol{D}} \boldsymbol{e} \tag{9}$$

where γ is a dimensionless scalar compliance parameter evolving from zero to infinity and

$$\hat{\boldsymbol{D}} = \begin{bmatrix} D_{nn} & 0 \\ 0 & D_{ss} \end{bmatrix} \tag{10}$$

is a stiffness matrix corresponding to a reference intermediate stage of the degradation process. Before crack initiation, the value of γ is zero. For simplicity, it is assumed here that crack initiation is controlled by the Rankine criterion of maximum principal stress. This means that the discontinuity line is inserted perpendicular to the direction of maximum principal stress, and the shear traction at the instant of crack initiation is zero.

The evolution of γ is described by the loading/unloading conditions in the Kuhn-Tucker form,

$$\dot{\gamma} \geq 0, \quad f \leq 0, \quad \dot{\gamma} f = 0 \tag{11}$$

The loading function f characterizing the elastic domain is defined as

$$f(\boldsymbol{e}, \gamma) \equiv F(\tilde{e}(\boldsymbol{e})) - \gamma \tag{12}$$

where F is a suitable function of the equivalent separation, $\tilde{e}$, which itself is a scalar measure of the separation vector $\boldsymbol{e}$. In [15] it has been proposed to set

$$\tilde{e} = \sqrt{\frac{\boldsymbol{e}^T \hat{\boldsymbol{D}} \boldsymbol{e}}{D_{nn}}} \tag{13}$$

and

$$F(\tilde{e}) = \frac{D_{nn} \tilde{e}}{g(\tilde{e})} \tag{14}$$

where g is a scalar function describing the traction-separation curve for Mode-I cracking.

3.2 Uniqueness of Element Response

Let us now explore under which conditions the element gives a unique response in the sense that, for any given evolution of the nodal displacements, the basic equations have a unique solution. Combining (7) with (9), we obtain after simple manipulations

$$(\hat{\boldsymbol{D}} + \gamma \boldsymbol{A} \boldsymbol{H}) \boldsymbol{e} - \gamma \boldsymbol{A} \boldsymbol{d} = \boldsymbol{0} \tag{15}$$

and differentiation with respect to time leads to

$$(\hat{\boldsymbol{D}} + \gamma \boldsymbol{A}\boldsymbol{H})\dot{\boldsymbol{e}} + \dot{\gamma}\boldsymbol{A}(\boldsymbol{H}\boldsymbol{e} - \boldsymbol{d}) = \gamma \boldsymbol{A}\dot{\boldsymbol{d}} \tag{16}$$

The central problem to be studied here is whether, for a given current state and for an arbitrary displacement rate, $\dot{\boldsymbol{d}}$, the rate equation (16) along with the loading/unloading conditions (11) has a unique solution for the separation rate, $\dot{\boldsymbol{e}}$, and for the rate of the compliance parameter, $\dot{\gamma}$.

1. If the current value of the loading function $f(\boldsymbol{e}, \gamma)$ is negative, it follows from the last loading/unloading condition (11) that the compliance parameter γ must remain constant. Equations (16) then lead to a unique solution for the rate of separation vector,

   $$\dot{\boldsymbol{e}} = \gamma(\hat{\boldsymbol{D}} + \gamma \boldsymbol{A}\boldsymbol{H})^{-1}\boldsymbol{A}\dot{\boldsymbol{d}} \tag{17}$$

   provided that the matrix $\hat{\boldsymbol{D}} + \gamma \boldsymbol{A}\boldsymbol{H}$ is regular. The rates of all other variables ($\dot{\boldsymbol{\varepsilon}}$, $\dot{\boldsymbol{\sigma}}$, $\dot{\boldsymbol{t}}$, and $\dot{\boldsymbol{f}}_{int}$) can be evaluated by simple substitution into the rate forms of (1), (3), (4), and (6).

2. Consider the more complicated situation when the current value of f is zero. In this case, the element can either unload elastically, or suffer additional damage. The former sub-case is characterized by $\dot{\gamma} = 0$ and $\dot{f} \le 0$, the latter by $\dot{\gamma} \ge 0$ and $\dot{f} = 0$.

   (a) If damage does not grow, the rate of separation vector is again given by (17). The solution is admissible only if

   $$\dot{f} \equiv \left(\frac{\partial F}{\partial \boldsymbol{e}}\right)^T \dot{\boldsymbol{e}} - \dot{\gamma} \equiv \gamma \boldsymbol{f}^T(\hat{\boldsymbol{D}} + \gamma \boldsymbol{A}\boldsymbol{H})^{-1}\boldsymbol{A}\dot{\boldsymbol{d}} \le 0 \tag{18}$$

   where $\boldsymbol{f} \equiv \partial F/\partial \boldsymbol{e}$.

   (b) If damage grows, we have to consider $\dot{\gamma}$ as an unknown and impose the consistency condition,

   $$\dot{f} = \boldsymbol{f}^T\dot{\boldsymbol{e}} - \dot{\gamma} = 0 \tag{19}$$

   Substituting $\dot{\gamma} = \boldsymbol{f}^T\dot{\boldsymbol{e}}$ into (16) we obtain a set of equations

   $$\left[\hat{\boldsymbol{D}} + \gamma \boldsymbol{A}\boldsymbol{H} + \boldsymbol{A}(\boldsymbol{H}\boldsymbol{e} - \boldsymbol{d})\boldsymbol{f}^T\right]\dot{\boldsymbol{e}} = \gamma \boldsymbol{A}\dot{\boldsymbol{d}} \tag{20}$$

   The solution

   $$\dot{\boldsymbol{e}} = \gamma\left[\hat{\boldsymbol{D}} + \gamma \boldsymbol{A}\boldsymbol{H} + \boldsymbol{A}(\boldsymbol{H}\boldsymbol{e} - \boldsymbol{d})\boldsymbol{f}^T\right]^{-1}\boldsymbol{A}\dot{\boldsymbol{d}} \tag{21}$$

   is admissible only if

   $$\dot{\gamma} \equiv \boldsymbol{f}^T\dot{\boldsymbol{e}} \equiv \gamma \boldsymbol{f}^T\left[\hat{\boldsymbol{D}} + \gamma \boldsymbol{A}\boldsymbol{H} + \boldsymbol{A}(\boldsymbol{H}\boldsymbol{e} - \boldsymbol{d})\boldsymbol{f}^T\right]^{-1}\boldsymbol{A}\dot{\boldsymbol{d}} \ge 0 \tag{22}$$

To prove uniqueness, we have to show that conditions (18) and (22) are complementary in the sense that, for an arbitrary displacement rate $\dot{\boldsymbol{d}}$, either one of the conditions holds as a strict inequality while the other one is violated, or both conditions hold as an equality (which is the neutral case). As γ cannot be negative, it is sufficient to demonstrate the complementarity of conditions

$$\boldsymbol{f}^T(\hat{\boldsymbol{D}}+\gamma\boldsymbol{A}\boldsymbol{H})^{-1}\boldsymbol{A}\dot{\boldsymbol{d}} \;\leq\; 0 \tag{23}$$

$$\boldsymbol{f}^T\left[\hat{\boldsymbol{D}}+\gamma\boldsymbol{A}\boldsymbol{H}+\boldsymbol{A}(\boldsymbol{H}\boldsymbol{e}-\boldsymbol{d})\boldsymbol{f}^T\right]^{-1}\boldsymbol{A}\dot{\boldsymbol{d}} \;\geq\; 0 \tag{24}$$

The proof is based on the Sherman-Morrison-Woodbury formula, which in general states that

$$(\boldsymbol{X}+\boldsymbol{Y}\boldsymbol{Z})^{-1}=\boldsymbol{X}^{-1}-\boldsymbol{X}^{-1}\boldsymbol{Y}(\boldsymbol{I}+\boldsymbol{Z}\boldsymbol{X}^{-1}\boldsymbol{Y})^{-1}\boldsymbol{Z}\boldsymbol{X}^{-1} \tag{25}$$

provided that the matrices $\boldsymbol{X}$, $\boldsymbol{Y}$, and $\boldsymbol{Z}$ are such that all operations make sense. In our case, we substitute $\boldsymbol{X}=\hat{\boldsymbol{D}}+\gamma\boldsymbol{A}\boldsymbol{H}$, $\boldsymbol{Y}=\boldsymbol{A}(\boldsymbol{H}\boldsymbol{e}-\boldsymbol{d})$, and $\boldsymbol{Z}=\boldsymbol{f}^T$, and we multiply the identity from the left by $\boldsymbol{f}^T$ and from the right by $\boldsymbol{A}\dot{\boldsymbol{d}}$. After some algebra we arrive at

$$\boldsymbol{f}^T\left[\hat{\boldsymbol{D}}+\gamma\boldsymbol{A}\boldsymbol{H}+\boldsymbol{A}(\boldsymbol{H}\boldsymbol{e}-\boldsymbol{d})\boldsymbol{f}^T\right]^{-1}\boldsymbol{A}\dot{\boldsymbol{d}}=\frac{\boldsymbol{f}^T\left(\hat{\boldsymbol{D}}+\gamma\boldsymbol{A}\boldsymbol{H}\right)^{-1}\boldsymbol{A}\dot{\boldsymbol{d}}}{1+\boldsymbol{f}^T\left(\hat{\boldsymbol{D}}+\gamma\boldsymbol{A}\boldsymbol{H}\right)^{-1}\boldsymbol{A}(\boldsymbol{H}\boldsymbol{e}-\boldsymbol{d})} \tag{26}$$

Consequently, the left-hand sides of (23) and (24) have the same sign, provided that the denominator in the fraction on the right-hand side of (26) is positive. If this is the case, conditions (23) and (24) are indeed complementary, because the inequality signs have the opposite sense. So it remains to check whether

$$\boldsymbol{f}^T\left(\hat{\boldsymbol{D}}+\gamma\boldsymbol{A}\boldsymbol{H}\right)^{-1}\boldsymbol{A}(\boldsymbol{d}-\boldsymbol{H}\boldsymbol{e})<1 \tag{27}$$

It follows from (15) that the term $\boldsymbol{A}(\boldsymbol{d}-\boldsymbol{H}\boldsymbol{e})$ can be replaced by $\hat{\boldsymbol{D}}\boldsymbol{e}/\gamma$. During continued loading the loading function f remains equal to zero and, consequently, $\gamma=D_{nn}\tilde{e}/g(\tilde{e})$; cf. equations (12) and (14). In addition, differentiating (14) and (13) we get

$$\boldsymbol{f}=\frac{\partial F}{\partial\boldsymbol{e}}=\frac{\mathrm{d}F}{\mathrm{d}\tilde{e}}\frac{\partial\tilde{e}}{\partial\boldsymbol{e}}=D_{nn}\frac{g(\tilde{e})-\tilde{e}g'(\tilde{e})}{g^2(\tilde{e})}\frac{\partial}{\partial\boldsymbol{e}}\sqrt{\frac{\boldsymbol{e}^T\hat{\boldsymbol{D}}\boldsymbol{e}}{D_{nn}}}=\frac{g(\tilde{e})-\tilde{e}g'(\tilde{e})}{\tilde{e}g^2(\tilde{e})}\hat{\boldsymbol{D}}\boldsymbol{e} \tag{28}$$

Condition (27) can be rewritten as

$$\frac{g(\tilde{e})-\tilde{e}g'(\tilde{e})}{\tilde{e}g^2(\tilde{e})}\boldsymbol{e}^T\hat{\boldsymbol{D}}\left(\hat{\boldsymbol{D}}+\frac{D_{nn}\tilde{e}}{g(\tilde{e})}\boldsymbol{A}\boldsymbol{H}\right)^{-1}\hat{\boldsymbol{D}}\boldsymbol{e}\frac{g(\tilde{e})}{D_{nn}\tilde{e}}<1 \tag{29}$$

Recall that $\tilde{e}$ is a function of the separation vector $\boldsymbol{e}$. So the left-hand side of (29) depends on $\boldsymbol{e}$ in a complicated manner and it is difficult to find its maximum value, representing

the most dangerous case. However, denoting $\hat{\boldsymbol{I}} = (\hat{\boldsymbol{D}}/D_{nn})^{-1/2}$ and $\boldsymbol{\nu} = \hat{\boldsymbol{I}}^{-1}\boldsymbol{e}/\tilde{e}$ and replacing $\hat{\boldsymbol{D}}$ by $D_{nn}\hat{\boldsymbol{I}}^{-2}$ and $\boldsymbol{e}$ by $\tilde{e}\hat{\boldsymbol{I}}\boldsymbol{\nu}$, condition (29) can be converted into

$$\chi(\tilde{e},\boldsymbol{\nu}) \equiv \left(1 - \frac{\tilde{e}g'(\tilde{e})}{g(\tilde{e})}\right)\boldsymbol{\nu}^T\left(\boldsymbol{I} + \frac{\tilde{e}}{g(\tilde{e})}\hat{\boldsymbol{I}}\boldsymbol{A}\boldsymbol{H}\hat{\boldsymbol{I}}\right)^{-1}\boldsymbol{\nu} < 1 \tag{30}$$

where $\boldsymbol{I}$ is a unit matrix. The advantage here is that the dependence on $\boldsymbol{e}$ is now replaced by the dependence on $\boldsymbol{\nu}$, which is a unit vector indirectly characterizing the direction of $\boldsymbol{e}$, and on $\tilde{e}$, which is a scalar related to the magnitude of $\boldsymbol{e}$ (measured in the metric induced by $\hat{\boldsymbol{I}}^{-2}$). When looking for an upper bound on $\chi(\tilde{e},\boldsymbol{\nu})$, we first maximize the quadratic form

$$q(\boldsymbol{\nu}) \equiv \boldsymbol{\nu}^T\left(\boldsymbol{I} + \frac{\tilde{e}}{g(\tilde{e})}\hat{\boldsymbol{I}}\boldsymbol{A}\boldsymbol{H}\hat{\boldsymbol{I}}\right)^{-1}\boldsymbol{\nu} = \boldsymbol{\nu}^T\left(\boldsymbol{I} + \eta\boldsymbol{Q}\right)^{-1}\boldsymbol{\nu} \tag{31}$$

over all unit vectors $\boldsymbol{\nu}$, with $\eta = \tilde{e}/g(\tilde{e})$ playing the role of a positive parameter. For brevity we have introduced a matrix $\boldsymbol{Q} = \hat{\boldsymbol{I}}\boldsymbol{A}\boldsymbol{H}\hat{\boldsymbol{I}}$. Note that this matrix is in general not symmetric. However, we will assume that $\boldsymbol{Q}$ is positive in the sense that

$$\boldsymbol{x}^T\boldsymbol{Q}\boldsymbol{x} \geq 0 \tag{32}$$

for any column matrix $\boldsymbol{x}$. For 2×2 matrices it is possible to derive the following estimate (see Appendix A):

$$\max_{\|\boldsymbol{\nu}\|=1} q(\boldsymbol{\nu}) = \frac{1 + \eta(\operatorname{tr}\boldsymbol{Q} - q_{min})}{1 + \eta\operatorname{tr}\boldsymbol{Q} + \eta^2\det\boldsymbol{Q}} \leq \frac{1}{1 + \eta\lambda_{min}(\boldsymbol{Q}_s)} \tag{33}$$

where

$$q_{min} = \min_{\|\boldsymbol{\nu}\|=1}\boldsymbol{\nu}^T\boldsymbol{Q}\boldsymbol{\nu} \tag{34}$$

and $\lambda_{min}(\boldsymbol{Q}_s)$ is the smallest eigenvalue of the symmetric part of $\boldsymbol{Q}$. We thus have, for any positive $\tilde{e}$ and any unit vector $\boldsymbol{\nu}$,

$$\chi(\tilde{e},\boldsymbol{\nu}) \leq \frac{1 - \dfrac{\tilde{e}g'(\tilde{e})}{g(\tilde{e})}}{1 + \dfrac{\tilde{e}}{g(\tilde{e})}\lambda_{min}(\boldsymbol{Q}_s)} \tag{35}$$

Due to the positiveness of $\boldsymbol{Q}$, its symmetric part is at least positive semidefinite, and $\lambda_{min}(\boldsymbol{Q}_s) \geq 0$. The denominator in (35) is therefore always positive, and a sufficient condition for $\chi(\tilde{e},\boldsymbol{\nu}) < 1$ is

$$1 - \frac{\tilde{e}g'(\tilde{e})}{g(\tilde{e})} < 1 + \frac{\tilde{e}}{g(\tilde{e})}\lambda_{min}(\boldsymbol{Q}_s) \tag{36}$$

Condition (36) is equivalent to

$$\lambda_{min}(\boldsymbol{Q}_s) > -H_{min} \tag{37}$$

where

$$H_{min} = \min_{\tilde{e}\geq 0} g'(\tilde{e}) \tag{38}$$

is the steepest slope of the traction-separation curve ($H_{min} < 0$ for softening). Recall that $\boldsymbol{Q} = \hat{\boldsymbol{I}}\boldsymbol{A}\boldsymbol{H}\hat{\boldsymbol{I}}$. The columns of matrix $\boldsymbol{A}\boldsymbol{H} = \boldsymbol{P}^T\boldsymbol{D}_e\boldsymbol{B}\boldsymbol{H}$ have the physical meaning of tractions on the crack line produced in an elastically responding element by unit displacements of the solitary node, and so this matrix reflects in a specific sense the stiffness of the element. Matrix $\hat{\boldsymbol{I}}$ is either a unit matrix (if the opening and sliding stiffnesses are equal), or a dimensionless diagonal matrix reflecting the ratio of the opening and sliding stiffness. The smallest eigenvalue of the symmetric part of $\boldsymbol{Q}$,

$$\lambda_{min}(\boldsymbol{Q}_s) = \min_{\|\boldsymbol{\nu}\|=1} \boldsymbol{\nu}^T\boldsymbol{Q}_s\boldsymbol{\nu} = \min_{\|\boldsymbol{\nu}\|=1} \boldsymbol{\nu}^T\boldsymbol{Q}\boldsymbol{\nu} \tag{39}$$

is a scalar measure of the elastic element stiffness relative to the given crack orientation. As H_{min} is negative, condition (37) is stronger than the condition that $\boldsymbol{Q}$ must be positive (which is equivalent to $\lambda_{min}(\boldsymbol{Q}_s) \geq 0$). This means that by making assumption (32) we did not restrict the range of admissible matrices $\boldsymbol{Q}$ more than is needed for uniqueness. It is also easy to show that if $\boldsymbol{Q}$ is positive then the matrix $\hat{\boldsymbol{D}}+\gamma\boldsymbol{A}\boldsymbol{H} = \hat{\boldsymbol{I}}^{-1}(D_{nn}\boldsymbol{I}+\gamma\boldsymbol{Q})\hat{\boldsymbol{I}}^{-1}$ cannot be singular (for $\gamma \geq 0$), which justifies its inversion appearing in (17).

3.3 Restriction on Element Size

It follows from dimensional analysis that

$$\lambda_{min}(\boldsymbol{Q}_s) = \theta\frac{E}{h} \tag{40}$$

where E is Young's modulus of the bulk material, h is some suitable measure of the element size, and θ is a dimensionless factor depending on the shape of the element, orientation of the discontinuity line and Poisson's ratio, but independent of the element size and Young's modulus. For example, for a one-dimensional element we obtain $\theta = 1$ if h is defined as the length of the element. Let us analyze the case of a triangular element under plane stress or plane strain. It is convenient to work in local coordinates aligned with the element side opposite to the solitary node; see Fig. 3. Matrices $\boldsymbol{H}$ and $\boldsymbol{P}$ are given by (2) and (5), resp. In order to cover both plane stress and plane strain, we write the elastic stiffness matrix in the form

$$\boldsymbol{D}_e = \begin{bmatrix} D_{11} & D_{12} & 0 \\ D_{12} & D_{11} & 0 \\ 0 & 0 & G \end{bmatrix} \tag{41}$$

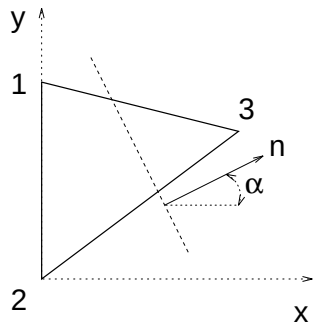

Figure 3: Choice of local coordinate system

in which $G = E/2(1+\nu)$ is the shear modulus, $D_{11} = 2G/(1-\nu)$ for plane stress, $D_{11} = 2G(1-\nu)/(1-2\nu)$ for plane strain, and $D_{12} = D_{11} - 2G$.

The strain-displacement matrix of a CST element is in general given by

$$\boldsymbol{B} = \frac{1}{2A}\begin{bmatrix} y_2-y_3 & 0 & y_3-y_1 & 0 & y_1-y_2 & 0 \\ 0 & x_3-x_2 & 0 & x_1-x_3 & 0 & x_2-x_1 \\ x_3-x_2 & y_2-y_3 & x_1-x_3 & y_3-y_1 & x_2-x_1 & y_1-y_2 \end{bmatrix} \tag{42}$$

where A is the area of the element and x_i, y_i, $i = 1, 2, 3$, are the nodal coordinates. In our special case, we set $x_1 = x_2 = 0$, $y_2 = 0$, and $A = y_1 x_3/2$, after which (42) simplifies to

$$\boldsymbol{B} = \frac{1}{y_1 x_3}\begin{bmatrix} -y_3 & 0 & y_3-y_1 & 0 & y_1 & 0 \\ 0 & x_3 & 0 & -x_3 & 0 & 0 \\ x_3 & -y_3 & -x_3 & y_3-y_1 & 0 & y_1 \end{bmatrix} \tag{43}$$

Combining (2), (5), and (41) with (43) we can evaluate the product

$$\boldsymbol{AH} = \boldsymbol{P}^T \boldsymbol{D}_e \boldsymbol{B} \boldsymbol{H} = \frac{1}{x_3}\begin{bmatrix} cD_{11} & -sD_{12} \\ -sG & cG \end{bmatrix} \tag{44}$$

Note that the only geometric characteristic of the element that appears here is the distance of the solitary node from the element side connecting the other two nodes, x_3.

For the sake of simplicity, let us assume that the diagonal stiffnesses in $\hat{\boldsymbol{D}}$ are the same, and so $\hat{\boldsymbol{I}}$ is a unit matrix. In this case, (44) is equal to the matrix $\boldsymbol{Q}$, and by eigenvalue analysis of its symmetric part we obtain

$$\lambda_{min}(\boldsymbol{Q}_s) = \frac{1}{2x_3}\left[c(D_{11}+G) - (D_{11}-G)\right] \tag{45}$$

As the elastic constants are proportional to Young's modulus, E, formula (45) indeed has the form (40), with the size of the element characterized by $h = x_3 =$ element height.

Factor θ is given by

$$\theta(\alpha,\nu) = \frac{c(3-\nu)-(1+\nu)}{4(1-\nu^2)} \tag{46}$$

for plane stress and

$$\theta(\alpha,\nu) = \frac{c(3-4\nu)-1}{4(1-2\nu)(1+\nu)} \tag{47}$$

for plane strain. Obviously, θ decreases with increasing deviation of the crack line from the direction parallel to an element side. Depending on the element shape and on the type of criterion used for positioning the discontinuity, it is possible to find the fan of crack directions that can separate the given node, and thus determine the minimum value of $c = \cos\alpha_{max}$ that can appear in the above formulae for θ. The corresponding value of $\theta(\alpha_{max},\nu)$ will be denoted as $\bar{\theta}(\nu)$. For example, for an equilateral triangle and a criterion placing the crack into the element center we have $\alpha_{max} = 30^\circ$ (see Fig. 4a), and $\bar{\theta}(\nu) = (0.3995 - 0.4665\nu)/(1-\nu^2)$ for plane stress. This is obviously positive for any thermodynamically admissible value of Poisson's ratio, $-1 \le \nu \le 0.5$. However, if the crack path is enforced to be continuous [16], angles up to $\alpha_{max} = 60^\circ$ can appear (see Fig. 4b), and $\bar{\theta}(\nu) = (0.125 - 0.375\nu)/(1-\nu^2)$ for plane stress. For materials with Poisson's ratio larger than 1/3, $\boldsymbol{Q}_s$ could have a negative eigenvalue (for certain unfavorable crack orientations), which would result into the loss of uniqueness, no matter how small the element is. For concrete, ν is usually between 0.1 and 0.2, and so $\bar{\theta}(\nu)$ remains positive. It may of course become negative if the element is severely distorted. Based on Fig. 4c it can be shown that, for triangles with all angles acute and with the ratio of the longest to the shortest side not exceeding a certain number β, the value of $\cos\alpha_{max}$ is not smaller than $1/\beta$, provided that the discontinuity is placed into the element center.

Inequality (37), which represents a sufficient condition of uniqueness on the element level, can now be reformulated in terms of the element size. It is assumed that the stress-

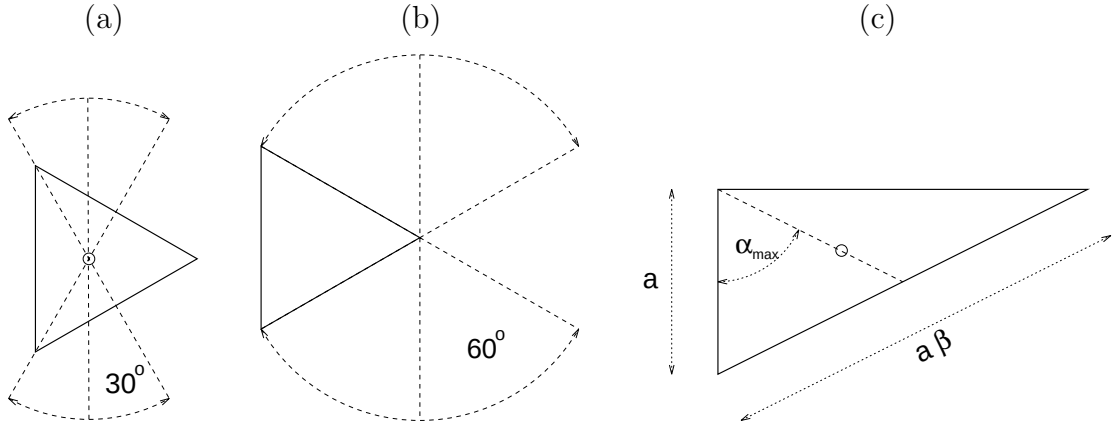

Figure 4: Fans of possible crack directions

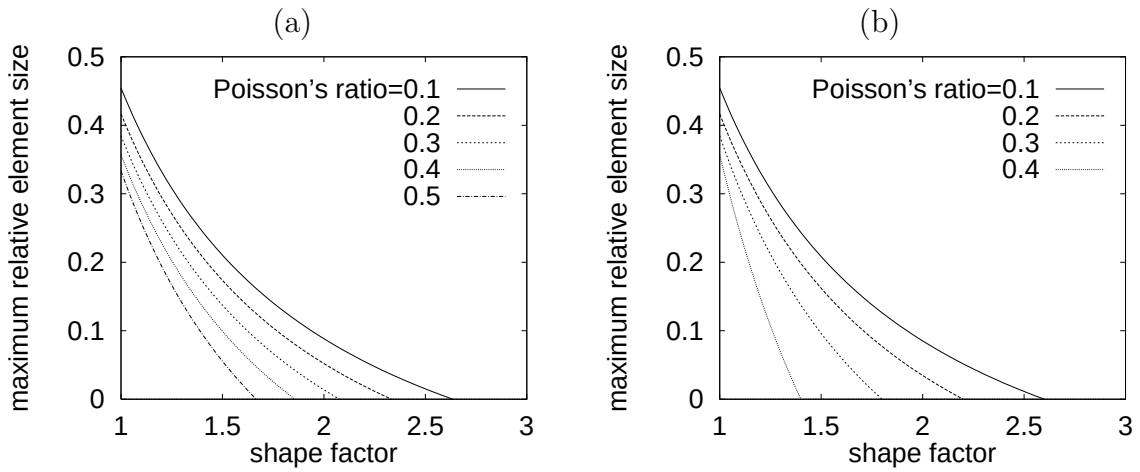

Figure 5: Maximum element size (relative to the characteristic length) as a function of the shape factor for a) plane stress, b) plane strain

separation curve is descending (softening), i.e., $H_{min} < 0$. The ratio $l_c \equiv -E/H_{min} = E/|H_{min}| > 0$ has the dimension of length and sets a certain characteristic length of the material model. Physically, l_c is the length of a bar for which the load-displacement diagram (under uniaxial tension) would have a vertical tangent at the steepest part of its softening branch. For example, for concrete C30 (according to the CEB code [17]) with Young's modulus $E_c = 29$ GPa, uniaxial tensile strength $f_{ctm} = 2.9$ MPa and fracture energy $G_F = 75$ Nm/m^2, the characteristic length is $l_c = E_c G_F / f_{ctm}^2 = 259$ mm, assuming that the softening curve is exponential. Using (40), condition (37) can be rewritten as

$$h < \bar{\theta}(\nu) l_c \tag{48}$$

If the element is sufficiently small (compared to the characteristic length of the material), its response is unique in the sense that for any prescribed evolution of nodal displacements the corresponding evolution of stresses and internal variables (such as the separation vector or the compliance parameter) is uniquely determined by the governing equations. Existence and uniqueness of the "exact" solution are necessary for a reliable performance of the numerical algorithm that evaluates the stresses and nodal forces. Fig. 5 shows the dependence of the factor $\bar{\theta}(\nu)$ on the shape factor β for selected values of Poisson's ratio, ν. Note that, due to (48), $\bar{\theta}(\nu) = h_{max}/l_c$ has the meaning of the maximum allowable element size normalized by the characteristic length. Obviously, the restriction on the element size becomes more severe with increasing values of Poisson's ratio and with increasing deviation of the element shape from the ideal case of an equilateral triangle.

4 PLASTICITY-TYPE TRACTION-SEPARATION LAW

4.1 Model Formulation

Consider now a different type of traction-separation law, this time formulated in the framework of plasticity. We introduce a yield function $f(\boldsymbol{t},\kappa)$ where κ is a scalar softening variable, defined by the rate equation

$$\dot{\kappa} = \boldsymbol{t}^T \dot{\boldsymbol{e}} \tag{49}$$

or

$$\dot{\kappa} = \|\dot{\boldsymbol{e}}\| \tag{50}$$

respectively corresponding to work softening and strain softening. For $f<0$, the current state is elastic and the crack opening remains constant. For $f=0$, the state is plastic and the evolution of the crack opening is dictated by the flow rule

$$\dot{\boldsymbol{e}} = \dot{\lambda}\boldsymbol{g}(\boldsymbol{t},\kappa) \tag{51}$$

where $\dot{\lambda}$ is the rate of the plastic multiplier and $\boldsymbol{g}$ is a suitable function specifying the direction of plastic flow. In the associated case we set $\boldsymbol{g} \equiv \partial f/\partial \boldsymbol{t}$. The loading/unloading conditions again assume the Kuhn-Tucker form,

$$f \le 0, \qquad \dot{\lambda} \ge 0, \qquad f\dot{\lambda} = 0 \tag{52}$$

This type of traction-separation law was used e.g. in [9], with

$$f(t_n,t_s,\kappa) = t_n^2 + \alpha_s t_s^2 - \sigma_e^2(\kappa) \tag{53}$$

and an associated flow rule. The softening variable κ was defined according to (50). In (53), α_s is a constant parameter weighting the relative influence of shear and normal traction, and $\sigma_e(\kappa)$ is a function describing the softening curve for pure Mode I, identical to function $g(\tilde{e})$ used by the damage-type model.

4.2 Uniqueness of Element Response

On the element level, the traction-separation law is exploited for the elimination of the separation $\boldsymbol{e}$ from the rate form of (7),

$$\dot{\boldsymbol{t}} = \boldsymbol{A}(\dot{\boldsymbol{d}} - \boldsymbol{H}\dot{\boldsymbol{e}}) \tag{54}$$

Similar to the analysis in Section 3.2, we can distinguish the following cases:

1. Elastic state, characterized by $f<0$.
   Both the plastic multiplier λ and the separation vector $\boldsymbol{e}$ remain constant, and the incremental behavior of the element is the same as if the element did not contain any discontinuity.

2. Plastic state, characterized by $f = 0$.
   The separation vector $\boldsymbol{e}$ either grows, in which case $\dot{f} = 0$ and $\dot{\lambda} \geq 0$, or becomes "frozen" due to unloading, in which case $\dot{f} \leq 0$ and $\dot{\lambda} = 0$.

   (a) In the former case, the rate of the plastic multiplier is computed from the consistency condition
   $$\dot{f} = \boldsymbol{f}_t^T \dot{\boldsymbol{t}} + f_\kappa \dot{\kappa} = 0 \tag{55}$$
   where $\boldsymbol{f}_t = \partial f / \partial \boldsymbol{t}$ and $f_\kappa = \partial f / \partial \kappa$. Substituting from (54), (50) and (51), we obtain
   $$\boldsymbol{f}_t^T \boldsymbol{A}(\dot{\boldsymbol{d}} - \boldsymbol{H}\boldsymbol{g}\dot{\lambda}) + f_\kappa \|\boldsymbol{g}\| \dot{\lambda} = 0 \tag{56}$$
   from which
   $$\dot{\lambda} = \frac{\boldsymbol{f}_t^T \boldsymbol{A} \dot{\boldsymbol{d}}}{\boldsymbol{f}_t^T \boldsymbol{A}\boldsymbol{H}\boldsymbol{g} - f_\kappa \|\boldsymbol{g}\|} \tag{57}$$
   The solution is admissible if $\dot{\lambda} \geq 0$.

   (b) In the case of unloading from a plastic state, the incremental behavior corresponds to a standard element, which means that $\dot{\boldsymbol{t}} = \boldsymbol{A}\dot{\boldsymbol{d}}$ and $\dot{\kappa} = 0$. The solution is admissible if
   $$\dot{f} = \boldsymbol{f}_t^T \dot{\boldsymbol{t}} + f_\kappa \dot{\kappa} = \boldsymbol{f}_t^T \boldsymbol{A} \dot{\boldsymbol{d}} \leq 0 \tag{58}$$

The incremental behavior is uniquely determined by the nodal displacement rates $\dot{\boldsymbol{d}}$ if cases a) and b) are complementary, i.e., if the denominator in (57) is positive. Thus, the condition of uniqueness reads

$$\boldsymbol{f}_t^T \boldsymbol{A}\boldsymbol{H}\boldsymbol{g} - f_\kappa \|\boldsymbol{g}\| > 0 \tag{59}$$

As an example, consider the quadratic yield condition (53). Introducing the matrix

$$\hat{\boldsymbol{I}} = \begin{bmatrix} 1 & 0 \\ 0 & \sqrt{\alpha_s} \end{bmatrix} \tag{60}$$

we can write the yield function as

$$f(\boldsymbol{t}, \kappa) = \boldsymbol{t}^T \hat{\boldsymbol{I}}^2 \boldsymbol{t} - \sigma_e^2(\kappa) \tag{61}$$

and evaluate its derivatives

$$\boldsymbol{f}_t = \frac{\partial f}{\partial \boldsymbol{t}} = 2\hat{\boldsymbol{I}}^2 \boldsymbol{t} \tag{62}$$

$$f_\kappa = \frac{\partial f}{\partial \kappa} = -2\sigma_e(\kappa)\sigma_e'(\kappa) \tag{63}$$

where $\sigma'_e = \mathrm{d}\sigma_e/\mathrm{d}\kappa$ is the derivative of the softening function, representing the softening modulus. For an associated flow rule we obtain

$$\boldsymbol{g} = \boldsymbol{f}_t = 2\hat{\boldsymbol{I}}^2\boldsymbol{t} \tag{64}$$

The uniqueness condition (59) then assumes the form

$$\chi(\boldsymbol{t},\kappa) \equiv \boldsymbol{t}^T\hat{\boldsymbol{I}}^2\boldsymbol{A}\boldsymbol{H}\hat{\boldsymbol{I}}^2\boldsymbol{t} + \sigma_e(\kappa)\sigma'_e(\kappa)\|\hat{\boldsymbol{I}}^2\boldsymbol{t}\| > 0 \tag{65}$$

Since uniqueness is being checked for case 2., e.g., for a plastic state satisfying the yield condition $f(\boldsymbol{t},\kappa) = 0$, we can replace $\sigma_e(\kappa)$ by $\|\hat{\boldsymbol{I}}\boldsymbol{t}\|$ and rewrite (65) as

$$\frac{\boldsymbol{t}^T\hat{\boldsymbol{I}}^2\boldsymbol{A}\boldsymbol{H}\hat{\boldsymbol{I}}^2\boldsymbol{t}}{\|\hat{\boldsymbol{I}}\boldsymbol{t}\|\,\|\hat{\boldsymbol{I}}^2\boldsymbol{t}\|} > -\sigma'_e(\kappa) \tag{66}$$

The left-hand side depends only on the direction of $\boldsymbol{t}$ and the right-hand side depends only on the softening variable κ, so condition (66) can be replaced by

$$\min_{\|\boldsymbol{\nu}\|=1} \frac{\boldsymbol{\nu}^T\boldsymbol{Q}\boldsymbol{\nu}}{\|\hat{\boldsymbol{I}}\boldsymbol{\nu}\|} > -H_{min} \tag{67}$$

where $\boldsymbol{Q} = \hat{\boldsymbol{I}}\boldsymbol{A}\boldsymbol{H}\hat{\boldsymbol{I}}$ and H_{min} is the minimum value of the softening modulus, corresponding to the steepest slope of the softening curve. To find the minimum of the expression on the left-hand side, we write the unit vector $\boldsymbol{\nu}$ as $\boldsymbol{\nu} = (\cos\phi, \sin\phi)$ and then minimize the resulting function with respect to the traction direction angle ϕ. In the special case when the parameter α_s from (53) is equal to 1, the minimum is equal to the smallest eigenvalue of the symmetric part of $\boldsymbol{Q}$, and we obtain exactly the same condition (37) as for the damage-type law with $D_{nn} = D_{ss}$.

Again, one can express the results in terms of the maximum element size as a function of the element shape factor. This is shown in Fig. 6 for several values of parameter α_s and for Poisson's ratio $\nu = 0.2$. The limit case $\alpha_s = 0$ should correspond to a Rankine-type model with only the normal traction taken into account. Surprisingly, for $\alpha_s \to 0$ the maximum element size tends to zero, independently of the element shape. This would mean that, for a Rankine-type model, there always exist states at which uniqueness of the element response is lost. However, this conclusion is not correct. It is important to take into account that as $\alpha_s \to 0$ the matrix $\hat{\boldsymbol{I}}$ tends to a singular matrix. For $\alpha_s = 0$, the left-hand side of (66) is equal to $t_n Q_{nn} t_n/|t_n|^2 = Q_{nn}$ where $Q_{nn} = cD_{11}/h$ is the first diagonal element of matrix $\boldsymbol{Q}$. In other words, vector $\hat{\boldsymbol{I}}\boldsymbol{t}$ does not have an arbitrary direction because its shear component vanishes, and the expression on the left-hand side of (67) should not be minimized over all unit vectors $\boldsymbol{\nu}$ but only evaluated for $\boldsymbol{\nu} = (1, 0)$. The resulting restriction on the element size is thus $h < h_{min} = -cD_{11}/H_{min}$, and for plane stress we obtain $h_{min}/l_c = 1/[(1-\nu^2)\beta]$. This restriction is much weaker than for any positive value of α_s, which indicates that the pure Rankine model is more robust than a penalty-like formulation of the general model with a quadratic yield condition and small value of α_s.

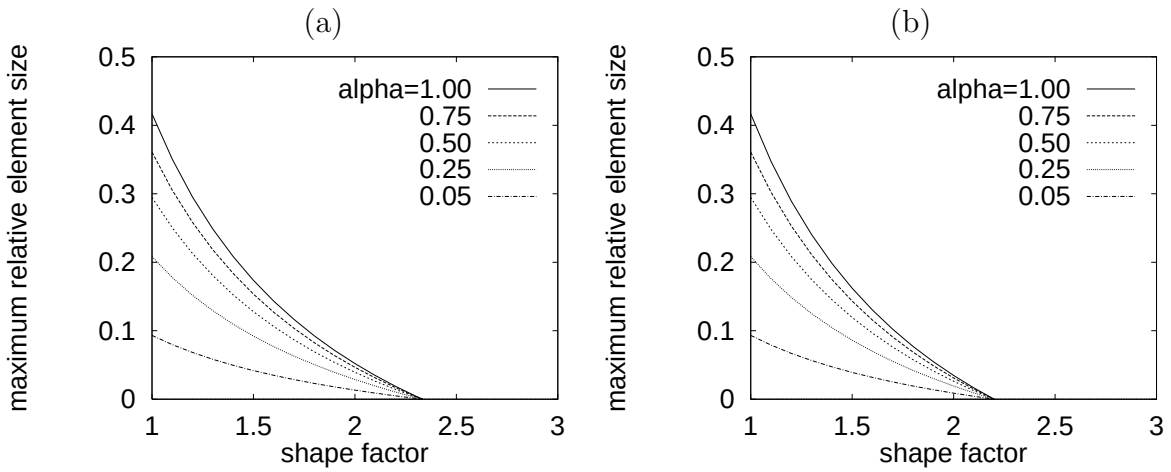

Figure 6: Maximum element size (relative to the characteristic length) as a function of the shape factor for a) plane stress, b) plane strain

5 CONCLUSION

This paper has presented a detailed analysis of the basic equations describing linear triangular finite elements with embedded displacement discontinuities that represent highly localized cracks. It has been shown that these equations have a unique solution only if the element size does not exceed a critical value that is affected by the characteristic length of the material, shape of the element, Poisson's ratio, and type of problem (plane stress or plane strain). If uniqueness is lost on the level of a single finite element, numerical problems resulting into the loss of convergence can be expected on the global level. The derived conditions permit the design of finite element meshes for which such problems do not occur.

Due to a limited size of this paper, the extensions of the present results to quadrilateral elements, smeared crack models, and multiple cracks are left for the conference presentation and for a future journal publication.

ACKNOWLEDGMENT

Financial support of the Swiss Committee for Technology and Innovation under project CTI.4424.1 is gratefully acknowledged.

REFERENCES

[1] M. Jirásek and Th. Zimmermann, 'Analysis of rotating crack model', *J. Eng. Mech.*, ASCE, **124** (1998), 842–851.

[2] A. R. Ingraffea, 'Discrete fracture propagation in rock: Laboratory tests and finite element analysis', PhD Dissertation, University of Colorado at Boulder, 1977.

[3] V. E. Saouma, 'Interactive finite element analysis of reinforced concrete: A fracture mechanics approach', PhD Dissertation, Cornell University, Ithaca, New York, 1981.

[4] J. Červenka, 'Discrete crack modeling in concrete structures', PhD Dissertation, University of Colorado at Boulder, 1994.

[5] M. Ortiz, Y. Leroy, and A. Needleman, 'A finite element method for localized failure analysis', *Comput. Meths. Appl. Mech. Eng.* **61**, 189–214 (1987).

[6] T. Belytschko, J. Fish, and B.E. Engelmann, 'A finite element with embedded localization zones', *Comput. Meths. Appl. Mech. Eng.* **70**, 59–89 (1988).

[7] E.N. Dvorkin, A.M. Cuitiño, and G. Gioia, 'Finite elements with displacement interpolated embedded localization lines insensitive to mesh size and distortions', *Int. J. Num. Meth. Eng.* **30**, 541–564 (1990).

[8] M. Klisinski, K. Runesson, and S. Sture, 'Finite element with inner softening band', *J. Eng. Mech.*, ASCE, **117**, 575–587 (1991).

[9] Th. Olofsson, M. Klisinski, and P. Nedar, 'Inner softening bands: A new approach to localization in finite elements', in *Computational Modelling of Concrete Structures*, ed. by H. Mang, N. Bićanić and R. de Borst, Pineridge Press, 1994, pp. 373–382.

[10] J.C. Simo and J. Oliver, 'A new approach to the analysis and simulation of strain softening in solids', in *Fracture and Damage in Quasibrittle Structures*, ed. by Z.P. Bažant et al., E. & F.N. Spon, London, 1994, pp. 25–39.

[11] M. Jirásek, 'Finite elements with embedded cracks ', LSC Internal Report 98/01, Swiss Federal Institute of Technology, Lausanne, April 1998.

[12] M. Jirásek, 'Embedded crack models for concrete fracture', Proc. *Computational Modelling of Concrete Structures* (EURO-C), ed. R. de Borst, N. Bicanic, H. Mang, and G. Meschke, Balkema, Rotterdam, 1998, pp. 291–300.

[13] M. Jirásek, 'Comparative study on finite elements with embedded discontinuities', *Comput. Methods Appl. Mech. Engrg.*, in press.

[14] J. Oliver, 'Modelling strong discontinuities in solid mechanics via strain softening constitutive equations. Part 1: Fundamentals. Part 2: Numerical simulation', *Int. J. Num. Meth. Eng.* **39**, 3575–3624 (1996).

[15] M. Jirásek and Th. Zimmermann, 'Embedded crack model: I. Basic formulation', *Int. J. Num. Meth. Eng.*, in press.

[16] M. Jirásek and Th. Zimmermann, 'Embedded crack model: II. Combination with smeared cracks', *Int. J. Num. Meth. Eng.*, in press.

[17] CEB-FIP Model Code 1990, Design Code, Thomas Telford, London, 1991.

APPENDIX A: UPPER BOUNDS ON A SPECIAL QUADRATIC FORM

The purpose of this Appendix is to derive an upper bound estimate for the quadratic form

$$q(\boldsymbol{\nu}) = \boldsymbol{\nu}^T \left(\boldsymbol{I} + \boldsymbol{Q}\right)^{-1} \boldsymbol{\nu} \tag{68}$$

where $\boldsymbol{Q}$ is a positive matrix. If $\boldsymbol{Q}$ is also symmetric then $\boldsymbol{I} + \boldsymbol{Q}$ is symmetric positive definite, and we can write

$$\max_{\|\boldsymbol{\nu}\|=1} q(\boldsymbol{\nu}) = \lambda_{max}\left(\left[\boldsymbol{I} + \boldsymbol{Q}\right]^{-1}\right) = \frac{1}{\lambda_{min}(\boldsymbol{I} + \boldsymbol{Q})} = \frac{1}{1 + \lambda_{min}(\boldsymbol{Q})} \tag{69}$$

where $\lambda_{max}(.)$ and $\lambda_{min}(.)$ denotes the largest and the smallest eigenvalue of a matrix. However, for nonsymmetric matrices we have to be more careful. If $\boldsymbol{Q}$ is a 2×2 matrix, it can be shown (based on the Caley-Hamilton theorem) that

$$\left(\boldsymbol{I} + \boldsymbol{Q}\right)^{-1} = \frac{1}{1 + \operatorname{tr}\boldsymbol{Q} + \det \boldsymbol{Q}} \left[(1 + \operatorname{tr}\boldsymbol{Q})\boldsymbol{I} - \boldsymbol{Q}\right] \tag{70}$$

and so

$$\boldsymbol{\nu}^T \left(\boldsymbol{I} + \boldsymbol{Q}\right)^{-1} \boldsymbol{\nu} = \frac{1}{1 + \operatorname{tr}\boldsymbol{Q} + \det \boldsymbol{Q}} \boldsymbol{\nu}^T \left[(1 + \operatorname{tr}\boldsymbol{Q})\boldsymbol{I} - \boldsymbol{Q}\right] \boldsymbol{\nu} = \frac{1 + \operatorname{tr}\boldsymbol{Q} - \boldsymbol{\nu}^T \boldsymbol{Q} \boldsymbol{\nu}}{1 + \operatorname{tr}\boldsymbol{Q} + \det \boldsymbol{Q}} \tag{71}$$

Thus, denoting

$$q_{min} = \min_{\|\boldsymbol{\nu}\|=1} \boldsymbol{\nu}^T \boldsymbol{Q} \boldsymbol{\nu} \tag{72}$$

we obtain

$$\max_{\|\boldsymbol{\nu}\|=1} q(\boldsymbol{\nu}) = \frac{1 + \operatorname{tr}\boldsymbol{Q} - q_{min}}{1 + \operatorname{tr}\boldsymbol{Q} + \det \boldsymbol{Q}} \tag{73}$$

Now let us replace matrix $\boldsymbol{Q}$ by its symmetric part, $\boldsymbol{Q}_s$. As $\boldsymbol{\nu}^T \boldsymbol{Q} \boldsymbol{\nu} = \boldsymbol{\nu}^T \boldsymbol{Q}_s \boldsymbol{\nu}$ for any $\boldsymbol{\nu}$, the value of q_{min} will not change. The trace of the symmetrized matrix is also the same

as the original one. So the only term in (73) that changes is the determinant. It is easy to prove that, for 2×2 matrices, $\det \boldsymbol{Q}_s \leq \det \boldsymbol{Q}$. Consequently, the expression on the right-hand side of (73) cannot decrease if the matrix is replaced by its symmetric part, and we obtain

$$\max_{\|\boldsymbol{\nu}\|=1} \boldsymbol{\nu}^T \left(\boldsymbol{I}+\boldsymbol{Q}\right)^{-1} \boldsymbol{\nu} \leq \max_{\|\boldsymbol{\nu}\|=1} \boldsymbol{\nu}^T \left(\boldsymbol{I}+\boldsymbol{Q}_s\right)^{-1} \boldsymbol{\nu} = \frac{1}{1+\lambda_{min}(\boldsymbol{Q}_s)} \tag{74}$$

The extension to 3×3 matrices is more difficult. Application of Caley-Hamilton theorem leads to

$$\left(\boldsymbol{I}+\boldsymbol{Q}\right)^{-1} = \frac{1}{1+\operatorname{tr}\boldsymbol{Q}+I_2(\boldsymbol{Q})+\det\boldsymbol{Q}} \left[(1+\operatorname{tr}\boldsymbol{Q}+I_2(\boldsymbol{Q}))\boldsymbol{I} - (1+\operatorname{tr}\boldsymbol{Q})\boldsymbol{Q}+\boldsymbol{Q}^2\right] \tag{75}$$

where $I_2(\boldsymbol{Q})$ is the second invariant (sum of principal minors) of $\boldsymbol{Q}$. The maximum of the quadratic form can now be expressed as

$$\max_{\|\boldsymbol{\nu}\|=1} \boldsymbol{\nu}^T \left(\boldsymbol{I}+\boldsymbol{Q}\right)^{-1} \boldsymbol{\nu} = \frac{(1+\operatorname{tr}\boldsymbol{Q}+I_2(\boldsymbol{Q}))\boldsymbol{I} - q_{min}}{1+\operatorname{tr}\boldsymbol{Q}+I_2(\boldsymbol{Q})+\det\boldsymbol{Q}} \tag{76}$$

where

$$q_{min} = \min_{\|\boldsymbol{\nu}\|=1} \left[(1+\operatorname{tr}\boldsymbol{Q})\boldsymbol{\nu}^T\boldsymbol{Q}\boldsymbol{\nu} - \boldsymbol{\nu}^T\boldsymbol{Q}^2\boldsymbol{\nu}\right] \tag{77}$$

This quantity is not easy to evaluate. It is also not clear whether symmetrization provides an upper bound similar to (74).

An alternative estimate, valid for any size of the problem, is based on the polar decomposition

$$\boldsymbol{I}+\boldsymbol{Q} = \boldsymbol{R}\boldsymbol{U} \tag{78}$$

where $\boldsymbol{R}$ is an orthogonal matrix and $\boldsymbol{U}$ is symmetric. We obtain

$$\begin{aligned} \boldsymbol{\nu}^T(\boldsymbol{I}+\boldsymbol{Q})^{-1}\boldsymbol{\nu} &= \boldsymbol{\nu}^T\boldsymbol{U}^{-1}\boldsymbol{R}^T\boldsymbol{\nu} \leq \lambda_{max}(\boldsymbol{U}^{-1}) = \frac{1}{\lambda_{min}(\boldsymbol{U})} = \frac{1}{\sqrt{\lambda_{min}(\boldsymbol{U}^2)}} = \\ &= \frac{1}{\sqrt{\lambda_{min}(\boldsymbol{I}+\boldsymbol{Q}+\boldsymbol{Q}^T+\boldsymbol{Q}^T\boldsymbol{Q})}} \leq \frac{1}{\sqrt{1+2\lambda_{min}(\boldsymbol{Q}_s)+\lambda_{min}(\boldsymbol{Q}^T\boldsymbol{Q})}} \end{aligned} \tag{79}$$